Soft Matter

RSC Publishing

PAPER

View Article Online
View Journal | View Issue

Cite this: *Soft Matter*, 2013, **9**, 7553

Staged self-assembly of PAMAM dendrimers into macroscopic aggregates with a microribbon structure similar to that of amelogenin†

Jiaojiao Yang,[a] Shuqin Cao,[a] Jiahui Li,[a] Jianyu Xin,[a] Xingyu Chen,[a] Wei Wu,[a] Fujian Xu[b] and Jianshu Li*[a]

Received 30th May 2013
Accepted 31st May 2013

DOI: 10.1039/c3sm51510a

www.rsc.org/softmatter

In this work, the PAMAM dendrimer self-assembles into macroscopic aggregates with a microribbon structure in aqueous solution containing ferric chloride, which are millimeters in length and micrometers in width. The microribbons have a stable structure with the thickness approaching 5 μm. Their self-assembly process and final morphology are pretty similar to those of the supramolecular assembly of amelogenin. The method opens a new avenue for fabricating novel and well-defined materials to mimic the assembly process of proteins and their biological functionalizations as protein analogues for wide applications.

Introduction

Self-assembly and disassembly of protein aggregates are fundamentals of many physiological functions,[1,2] and related to the pathogenesis,[3,4] prevention[5,6] and therapy of various diseases.[7,8] For instance, amelogenin protein, which can fold into a unique globular form that preserves a bipolar nature, was derived from its primary structure. It has a strong tendency to assemble into nanospheres and then form a birefringent microribbon structure, which are both vital steps for its function as a scaffolding protein for the tooth enamel biomineralization, especially in terms of controlling the oriented growth of apatite crystals.[9–11] Due to the difficulty of the extraction or purification of native proteins, it could be highly valuable to seek synthetic polymers which can mimic the self-assembly behavior and morphology of those proteins.

Dendrimers, which have well-defined spherical structures with monodispersity similar to proteins, are referred to as 'artificial proteins' by some researchers and have been studied widely in recent years.[12–14] These fundamental properties have led to the extensive use of dendrimers and their derivatives as protein analogues for biological, medicinal and material applications.[15–20] Also, the unique layered architecture of dendrimers provides them with the ability to morph into a variety of virtual supramolecular arrangements in response to external stimuli.[21–27] It has also been reported that dendrimers or dendrons could control the self-assembly of oppositely charged biomolecules, such as viruses and nucleic acids, all amenable to the so-called dendritic effects, and to the manner the dendritic scaffold reacts to intermolecular interactions.[28,29] Although the driving force of the assembly of dendrimers is different from that of proteins, they both have a well-defined higher structure and specific functions. Hence it is important to study the self-assembly process of dendrimers to obtain supramolecular aggregates, which may mimic that of proteins to generate functional materials.

Most interesting to us is the fact that, as supramolecular building blocks, dendrimers have a tendency to form multiple levels of hierarchies. For instance, in aqueous solution containing cadmium acetate ($Cd–(CH_3COO)_2$), fourth generation amino-terminated poly(propylene imine) dendrimers can form a functional nanofiber by the ion-selective controlled assembly method.[30–32] Meanwhile, the poly(amidoamine) (PAMAM) dendrimer has been widely used for self-assembly at the nanoscale.[33–35] It has been described to form fractal aggregates through electrostatic interactions between a 3.5 generation carboxylate terminated PAMAM dendrimer and a fourth generation amine terminated PAMAM dendrimer in aqueous solutions.[36] It has also been reported that uracil-functionalized PAMAM dendrimers can exhibit a hierarchical formation with an ordered dendritic structure on the micron length scale.[37] In addition, these dendrimer aggregates could act as functional templates for various applications, *e.g.*, crown-shaped platinum nanoparticles could be produced by ultraviolet irradiation using aggregates of fourth generation amine terminated PAMAM dendrimers in water.[38]

However, there is no report about the self-assembly process of PAMAM dendrimers as protein analogues under moderate conditions, which is important for their application in the area

[a]*College of Polymer Science and Engineering, Sichuan University, Chengdu 610065, P. R. China. E-mail: jianshu_li@scu.edu.cn*

[b]*College of Materials Science and Engineering, Beijing University of Chemical Technology, Beijing 100029, P. R. China*

† Electronic supplementary information (ESI) available: Additional Fig. S1–S10. See DOI: 10.1039/c3sm51510a

of bionics. In this work, we report that the carboxyl terminated PAMAM dendrimer could assemble into macroscopic aggregates with a microribbon structure, which is millimeters in length and micrometers in width. The self-assembly process is induced by ion chelation in aqueous solution, and undergoes a transition from nanospheres to nanosphere chains and a subsequent microribbon structure, which is similar to that of amelogenin. Since the morphology of assembled aggregates at different self-assembly stages is essential for the physiological functions of proteins,[2,9–11] this work could provide essential information about controlling the self-assembly process of PAMAM dendrimers as "amelogenin analogues" for wide applications.

Materials and methods

Materials

All common solvents and reagents were obtained from Tianjin Bodi Chemical Holding Company. Ethylenediamine was purified by reduced pressure distillation. Methyl acrylate was purified by passage through a column of activated basic alumina to remove the inhibitor. Chromatographic grade methanol was used as received. Ultrapure water produced from a Milli-pore system with a resistivity higher than 18.2 MΩ cm was used in all the experiments.

Syntheses and characterization of PAMAM-COOH dendrimers

G4.0 PAMAM dendrimer was synthesized step by step following the classical method reported by Tomalia *et al.*[17] Then, 0.45 g G4.0 PAMAM was dissolved in 15 mL DMSO under harsh dehydration conditions. 1.044 g butanedioic anhydride, dissolved in 15 mL DMSO, was added to the dendrimer solution and then reacted at 25 °C for 24 h. After being diluted with 50 mL deionized water, the solution was dialyzed (MWCO 3500) against water for 3 days and then lyophilized to yield the fourth-generation carboxyl terminated PAMAM dendrimers.

^{1}H NMR and matrix-assisted laser desorption/ionization time-of-flight mass spectrometry (MALDI-TOFMS) were used for characterization of G4.0 PAMAM-COOH.

Formation of PAMAM microribbons

Lyophilized G4.0 PAMAM was dissolved in different solvents at various concentrations. Table 1 shows several solution conditions with their initial ionic strength and temperature. When the concentration of iron ion is in the range of 1×10^{-4} to 1×10^{-2} mol L^{-1}, and the concentration of the dendrimer is in the range of 1 to 10 mg mL^{-1}, the water soluble G4.0-COOH PAMAM dendrimer could self-assemble into naked-eye visible aggregates within 18 hours.

Characterization of PAMAM microribbons

The samples were picked up by a needle and observed under a glass slide for further characterization. Polarization microscopy was performed with an Olympus BX-51. The optical microspectroscopy pattern for dendrimer ribbons was obtained using a Keyence VHX-1000 and an Optec BK-5000. The macroscopy was performed using a Canon 550D. X-ray diffraction analysis (Dmax 1400, 40 kV, 110 mA, Japan) was performed on the microribbon surface to examine the orientation degree.

Table 1 Conditions used for the formation of microribbons. The initial ionic strength and temperature of the solution

Dendrimer	$FeCl_3$	Temperature	Microribbon
1 mg mL^{-1}	No salt	25 °C	N
1 mg mL^{-1}	0.1 M	25 °C	N
1 mg mL^{-1}	0.01 M	25 °C	Y
1 mg mL^{-1}	0.001 M	25 °C	Y
1 mg mL^{-1}	0.0001 M	25 °C	Y
1 mg mL^{-1}	0.0001 M	4 °C	Y
1 mg mL^{-1}	0.0001 M	4 °C	Y
2 mg mL^{-1}	0.0001 M	25 °C	Y
5 mg mL^{-1}	0.0001 M	25 °C	Y
10 mg mL^{-1}	0.0001 M	25 °C	Y
25 mg mL^{-1}	0.0001 M	25 °C	N

Characterization of the formation process of PAMAM microribbons

Atomic force microscopy (AFM) was performed in tapping mode in air with a NanoScope MultiMode III AFM instrument. 20 μL of the solution was taken out and diluted to 2 mL using deionized water. The sample was prepared by dropping the 200 μL diluted solution on a quartz plate. Scanning electron microscope (SEM) observation of the microribbon sample was performed using a Hitachi S-450 operating at 15 kV. The samples were sputtered with Au after lyophilization. For transmission electron microscopy (TEM) experiments, the dendrimer solution samples (5 μL) were pipetted onto a carbon-coated electron microscopy grid and stained with 2% uranyl acetate for 20 minutes. After stoving, the samples were observed using a FEI TecnaiG2 F20 S-TWIN transmission electron microscope, operating at an accelerating voltage of 200 kV. Dynamic light scattering (DLS) measurement was carried out on a Brookhaven BI-200 SM system incorporating a He–Ne laser (λ = 532 nm) at 25 °C. The hydrodynamic diameters of dendrimer aggregates at a concentration of 1 mg mL^{-1} in water were collected two times at an angle of 90°. The hydrodynamic diameters of dendrimer microribbons at a concentration of 1 mg mL^{-1} in water were measured by dynamic light scattering (DLS, Zetasizer Nano, Malvern, UK) at angles of 90° and 30°.

Results and discussion

The syntheses of the PAMAM dendrimer and its carboxyl-terminated derivative *via* a step-by-step method were previously reported by Tomalia and Shi, respectively.[17,39] As shown in Fig. 1, ^{1}H NMR (400 Hz, $CDCl_3$) spectrometry shows the structure of G4.0 PAMAM dendrimers. The NMR peak assignments confirmed the formation of carboxyl-terminated PAMAM. The ratio of succinamic acids (c and d) to that of amino groups (a and b) indicates that 25 of 32 surface groups were modified to carboxyl groups. Matrix-assisted laser desorption/ionization

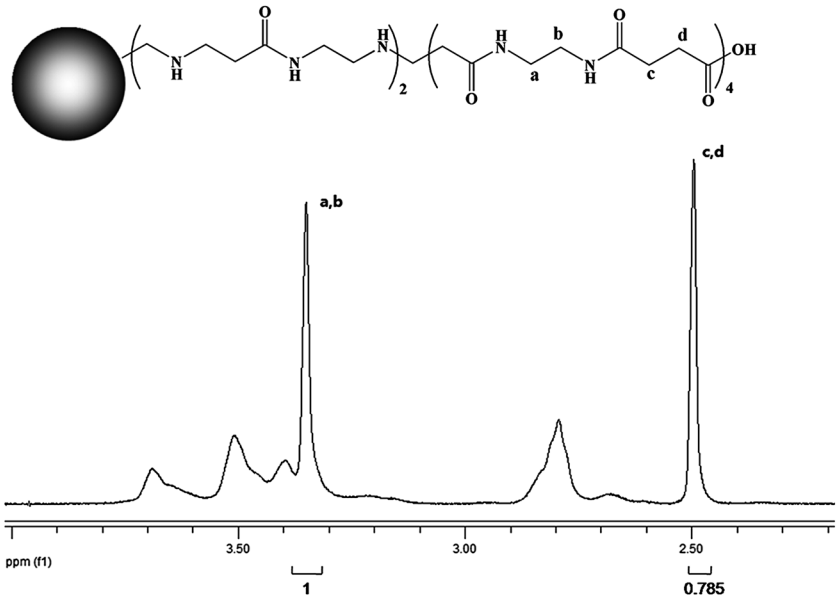

Fig. 1 ^{1}H NMR spectrum of the G4.0-COOH PAMAM dendrimer. The data show that 25 of 32 amino groups were modified to carboxyl groups.

time-of-flight mass spectrometry also shows that the theoretical M_w of G4-COOH is 10 100.

When the dendrimers were added to an aqueous solution of ferric chloride with varying concentrations (Table 1), microribbons were formed within 18 hours. Fig. 2 shows the typical morphology of the macroscopic aggregates with the microribbon structure. The photograph of the self-assembled objects shows naked eye-visible aggregates which are bundles of fibril-like units millimeters in length (Fig. 2a). The macroscopic fibers have inhomogeneous lengths and are tangled forming objects which have the longest length of 4.3 mm when using a high concentration of the G4.0-COOH PAMAM dendrimer (1 mg mL^{-1}). The morphology of the aggregates was also observed by optical microscopy. We could see that they are transparent and light yellow ribbons with a smooth surface structure and have a width of around 30 μm (Fig. 2b). It is noted that when the concentration of iron ion is higher than a certain concentration, the dendrimers could generate random aggregates and precipitate immediately due to the overwhelming ion interaction. When the concentration of dendrimers is lower than a certain critical concentration, there are not enough self-assembled materials to form microribbons. Meanwhile, when the concentration of dendrimers is very high and the concentration of iron is very low, the dendrimers also could not form microribbons. Within the scope of the investigation in this work, the appropriate concentrations of iron ion and dendrimers are in the range of 1×10^{-4} to 1×10^{-2} mol L^{-1} and 1 to 10 mg mL^{-1}, respectively (Table 1).

As shown in Fig. 3a, the microribbons formed by PAMAM dendrimers are dispersed randomly in the aqueous solution and the length of the microribbons is significantly different from their width. With the help of a super-depth 3D microscope, the thickness of a single ribbon could be calculated as around 5 μm (Fig. 3b). The light yellow color of the ribbons should be due to the iron ion and may vary according to different concentrations. The edge of the ribbons has some defects, which may be due to the sample preparation process or it may be the immature region of the self-assembled microribbons. The structure of mature aggregates with a microribbon

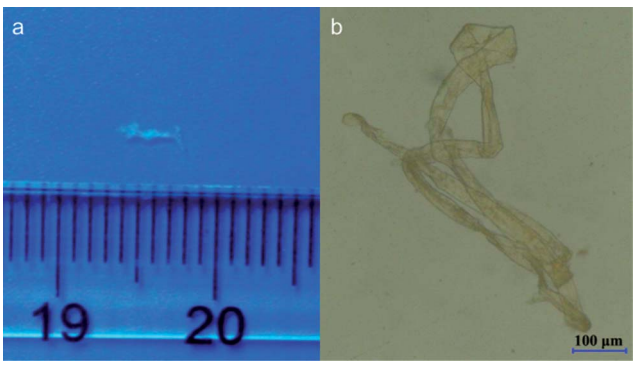

Fig. 2 The formation of macroscopic aggregates with a microribbon structure by the G4.0-COOH PAMAM dendrimer. The bundles of macroscopic objects were recorded by a digital camera (left) and super-depth 3D microscope (right).

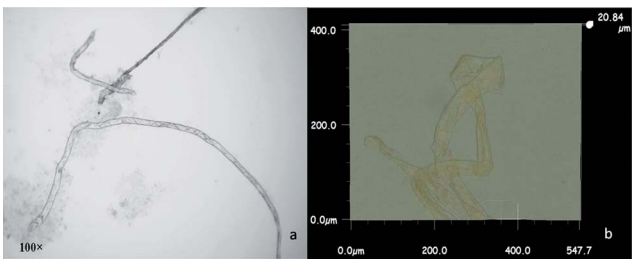

Fig. 3 Microscopy of PAMAM dendrimer micro-ribbons. (a) Using an optical microscope. The ribbons have different lengths but almost the same width. (b) Using a super-depth 3D microscope. The thickness of a single layer is about 5 μm.

structure could be maintained in the solution for more than one year in our lab. Meanwhile, it is also stable in many solvents such as hydrochloric acid, sodium hydroxide and sodium chloride, as well as in chelating agents (ethylenediaminetetraacetic acid, EDTA).

In order to examine the configuration of the microribbons, we observed the samples by polarization microscopy. It was previously reported that the structural arrangement *via* self-assembly of dendrimers or dendritic macromolecules was not crystalline.[36–38,40] Although the aggregates with the microribbon structure do not show birefringence under polarized light microscopy which indicates an amorphous structure (Fig. 4), their morphology is pretty similar to that of the supramolecular assembly of amelogenin.[9]

The visualization of the self-assembly process of dendrimers is very important for understanding the mechanism and seeking a method to obtain new materials. It is well known that a single PAMAM dendrimer molecule has a spherical structure and its size is in the range of nanometers, which is similar to that of quite a few globular proteins. Thus it could be an ideal building block to mimic the assembly process of protein supramolecular aggregates (especially for amelogenin in this work). Fig. 5 shows the assembly stages of G4.0-COOH PAMAM dendrimers. At the early stage, the monomer forms a nanosphere structure (Fig. 5a). Those nanospheres have a quasi-spherical appearance and some of them are bridged by a thin thread, which indicates their further evolution to the next stage of nanosphere chains (Fig. 5a, red circle). Then, the nanosphere chains fused with each other to form microfibers (Fig. 5c). The nanosphere chains and microfibers are both higher levels of hierarchical structures formed by separate nanospheres. As can be seen, the length of the microfiber was longer than 10 μm at these stages. And it is interesting to find that the microfiber was around 100 nm in width at 3 h but increased to around 1 μm at 10 h. Thus, we may speculate that the microfiber fused into a wider microribbon (Fig. 5d) with the increase of time.

The substructure of the nanosphere chain could be observed by AFM (Fig. 6a, arrow), which shows that the nanosphere chains were formed by fusion of the small nanospheres. Then, this nanosphere chain could be the precursor to form the microfibers. Meanwhile, the surface of the microfibers has been

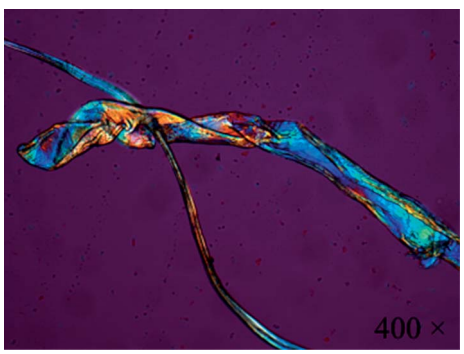

Fig. 4 Polarized light micrograph of PAMAM dendrimer microribbons. The ribbons do not show the birefringence and reveal an amorphous state.

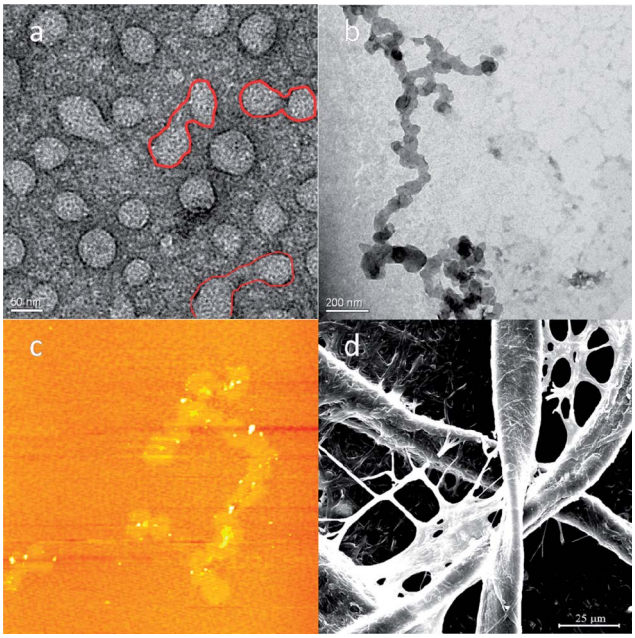

Fig. 5 Morphology characterization of the staged assembly process of the G4.0-COOH PAMAM dendrimer (1 mg mL^{-1}) in 0.0001 mol L^{-1} ferric chloride solution. (a) TEM micrograph of the dendrimer nanosphere formed at 1 h (scale bar: 50 nm). (b) TEM micrograph of the nanosphere chain formed at 3 h (scale bar: 200 nm). (c) AFM image of the larger nanomicrofiber chain formed at 10 h (image area: 10 × 10 μm^2). (d) SEM image of the mature aggregates with a microribbon structure formed at 18 h (scale bar: 25 μm).

observed by SEM (Fig. S1†). It is found that there are many nanospheres on the surface of the PAMAM microfibers, which could also support the hypothesis. The transition process from a microfiber to a microribbon has been studied, which could be solid evidence for the intermediate structure.[41] The intermediate object between the microfiber (Fig. 5c) and microribbon (Fig. 5d) is observed at 14 h as shown in Fig. 6b. The fusing bundles of microfibers are identified, which should be the precursors to form the following microribbon. It is worth noting that the microfibers in Fig. 6b are almost homogeneous, indicating that the assembly of the PAMAM dendrimer takes place in an ordered manner. As shown in Fig. 6c, there are quite a few microfibers (indicated by an arrow) on the microribbon surface, which could support the speculation that the microribbon is formed by microfibers.

To further investigate the intermediate states and the formation of the microribbons, we analyzed the particle size change of the G4.0-COOH dendrimer by dynamic light scattering analysis (DLS) in aqueous solution (Fig. 7, some important discrete points of the measured data are presented in Fig. S2†). Overall, the size of the PAMAM dendrimer increased gradually with the increase of time. With the increase of time from 0 to 50 min, the D_H of the G4.0 PAMAM-COOH dendrimer increases from 4 to 24 nm. Monomers and oligomers such as dimers and trimers of G4.0-COOH could be detected in the solution as indicated by the size measurement. At this stage, since there are quite a few monomers and iron ions in aqueous solution, a lot of oligomers could be produced. Then, almost all

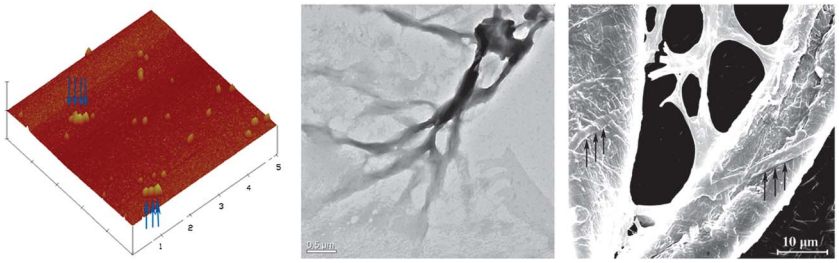

Fig. 6 Images of subunits of nanospheres and microribbons. (a) AFM image of the surface of PAMAM dendrimer nanosphere chains (image area: 5 × 5 μm^2). (b) SEM image of PAMAM dendrimer aggregates at 14 h. (c) SEM image of the surface of the PAMAM dendrimer ribbons (scale bar: 10 μm).

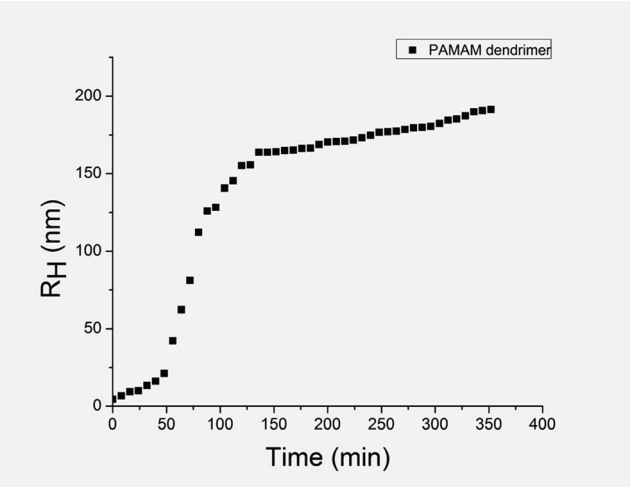

Fig. 7 Representative DLS autocorrelation curves of G4.0-COOH PAMAM dendrimer solutions (dendrimer: 1 mg mL^{-1}, ferric chloride: 0.0001 mol L^{-1}).

the monomers were transformed into oligomers, thus the D_H of the aggregates exhibited a rapid growth from 24 to 160 nm with the increase of time from 50 to 130 min, which may be due to the combination of oligomers. After that, the D_H of the aggregates did not exhibit an obvious increase. At this stage, the nanospheres formed by aggregates of oligomers could become the assembly units for further hierarchical structures of nanosphere chains. Also, the transition of the PAMAM dendrimer from the microfiber to ribbon was measured by dynamic light scattering at two angles (Fig. S3,† 30 °C and 90 °C). Since DLS is usually used to measure the diameters of small spherical particles, the diameters of the microfiber and microribbon measured by DLS can only provide some additional information. As shown in Fig. S3,† there are 4 peaks of the PAMAM dendrimer at this time point, which shows the characteristic of unsymmetrical assemblies.

Also, the effects of dendrimer generations on the assembled morphology have been investigated. When G3.0-COOH PAMAM dendrimers (1.0 mg mL^{-1}, the optimized concentration as that of G4.0-COOH PAMAM) were dissolved in aqueous 1×10^{-4} mol L^{-1} iron ion, macroscopic aggregates could also be formed. Using a super-depth 3D microscope, we could see that the macroscopic aggregates are composed of bundles of microfibers, the size of which is much smaller than that formed by G4.0-COOH PAMAM (Fig. S4†). We speculate that G3.0-COOH PAMAM dendrimers have a smaller size and fewer surface groups than those of G4.0-COOH PAMAM dendrimers, thus the morphology of macroscopic aggregates formed by them could have some difference, which is consistent with previous reports.[31] As we know, pH value is an important parameter to influence the assembly process of macromolecules in many systems. Thus, the self-assembly of the PAMAM dendrimer was also studied at different pH values (pH = 3, 7, 11). As shown in Fig. S5,† similar morphologies of PAMAM dendrimer aggregates have been obtained in the three systems. This is because the chelation of the PAMAM dendrimer and iron ion is the self-assembly driving force of the system and pH changes cannot affect the concentration of PAMAM dendrimers and iron ion, thus similar morphologies of PAMAM dendrimer aggregates could be formed at different pH conditions.

It is very important to reveal the role of metal ions and anions in the self-assembly process. Within the scope of our investigation, the G4.0-COOH PAMAM dendrimer could also self-assemble into macroscopic aggregates in an aqueous solution of other ions such as $CuCl_2$ (Fig. S6†) and $AlCl_3$ (Fig. S7†), but they could not form the microribbon structure as in $FeCl_3$ solution. As can be seen, G4.0-COOH dendrimers self-assembled into platy aggregates in aqueous solution of $CuCl_2$ and into irregular microscopic aggregates in an aqueous solution of $AlCl_3$, respectively (Fig. S6 and S7†). It is interesting to find that G4.0-COOH dendrimers could self-assemble into regular sheet-like morphology in an aqueous solution of $CaCl_2$ (Fig. S8†), which provides the possibility for potential application in the biomineralization field. Meanwhile, the G4.0-COOH PAMAM dendrimers could form macroscopic aggregates with microribbon structures in aqueous solution of $Fe(NO_3)_3$ (Fig. S9†) as that in $FeCl_3$ solution. All the above experiments indicated that it is the type of metal ion (Fe^{3+}), instead of the type of anion, that plays an important role in the self-assembly of G4.0-COOH PAMAM dendrimers into macroscopic aggregates with a microribbon structure.

The proposed mechanism of microribbon formation is shown schematically in Fig. 8. The carboxyl groups at the surface of the G4.0-COOH PAMAM dendrimer provide the chelation sites with the metal ion. When the G4.0-COOH PAMAM dendrimer is added to an aqueous solution of ferric chloride, the Fe^{III} cations coordinate to the peripheral

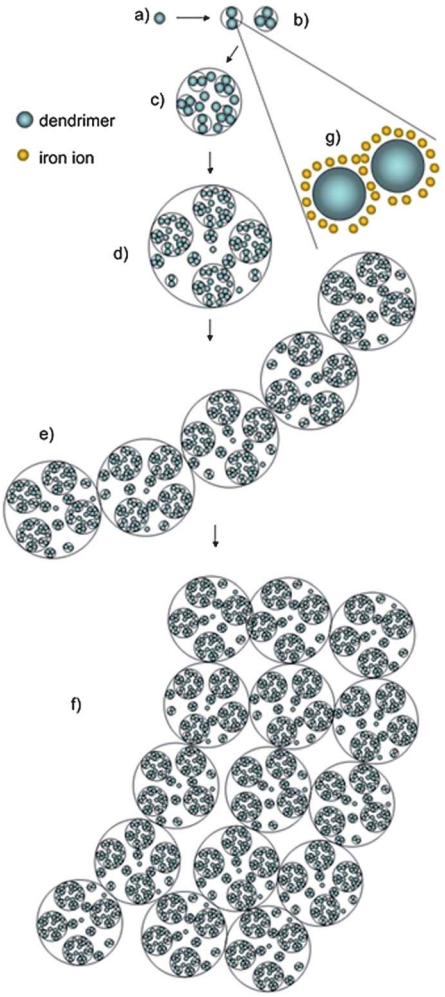

Fig. 8 Schematic illustration of the self-assembly process of G4.0-COOH PAMAM. (a) The single G4.0-COOH PAMAM dendrimer molecule is a globular unit. R_h = 4.4 nm. (b and c) Oligomer of G4.0-COOH PAMAM dendrimers. R_h = 6–10 nm and 40–80 nm for different stages. (d) Nanosphere structures are formed through the association of oligomers and monomers. R_h = 160–200 nm. (e) Further association of nanospheres results in a larger assembly to form nanosphere chains. (f) The organization of the nanosphere chain to form a microribbon structure. (g) Interconnection of G4.0-COOH PAMAM dendrimers by iron ion chelation.

carboxylate radical anions to form nanospheres, the size of which is gradually increased in the process of self-assembly as revealed by DLS data (Fig. 7). These Fe^{III} cations act as a linker between dendrimers in aqueous solution and promote the self-assembly process. Because only 25/32 of the surface groups were modified into carboxyl groups, the ion chelation density between the G4.0-COOH dendrimer and Fe^{III} should be heterogeneous in different directions.[30–32] Also, the flexibility of the dendrimer should be a key parameter for its self-assembly with a preferential directionality.[42] Thus, the nanospheres may reorganize into nanosphere chain structures (precursors of microfibers) instead of bigger spheres as shown in Fig. 8e. As shown in Fig. S10,† the PAMAM microribbon shows amorphous character in the XRD measurement, which is consistent with the result of polarization microscopy. Thus we can say that the PAMAM microribbon is formed by the redistribution of microfibers,[43] but does not exhibit crystallization although it is present in an orderly manner. Interestingly, the self-assembly process of the G4.0-COOH PAMAM dendrimer is also similar to that of proteins such as amelogenin, which could be another piece of evidence to define dendrimers as artificial proteins.[9]

Conclusions

We demonstrate that carboxyl terminated PAMAM dendrimers have a strong tendency to self-assemble into hierarchical structures with the morphology of nanospheres, subsequent nanosphere chains and microfibers, and finally macroscopic aggregates consisting of microribbons, which is similar to that of amelogenin. In our recent work, we further found that the PAMAM dendrimer could successfully act as the analogue of amelogenin to induce *in situ* biomineralization of human tooth enamel.[44] The facile method to prepare microribbons of PAMAM dendrimers in the presence of iron ions opens a new avenue for fabricating novel and well-defined materials as protein analogues to mimic the assembly process of proteins and their biological functionalizations for wide applications.

Conflict of interest

The authors declare no competing financial interest.

Acknowledgements

Financial support from the National Natural Science Foundation of China (51073102), Fok Ying Tung Education Foundation (122034), Program for New Century Excellent Talents in University (NCET-10-0592), Program for Changjiang Scholars and Innovative Research Team in University (IRT1163), Foundations of Sichuan Province (2012JQ0009), Fundamental Research Funds for the Central Universities (2010SCU22001, 2011SCU04A04) and Natural Science Foundation of Jiangsu Province (BK2010248, BK2011340) is gratefully acknowledged.

References

1 R. Kayed, E. Head, J. L. Thompson, T. M. Mclntire, S. C. Milton, C. W. Cotman and C. G. Glabe, *Science*, 2003, **300**, 486–489.
2 G. He, T. Dahl, A. Veis and A. George, *Nat. Mater.*, 2003, **2**, 552–558.
3 M. Bucciantini, E. Giannoni, F. Chiti, F. Baroni, L. Formigli, J. Zurdo, N. Taddei, G. Ramponi, C. M. Dobson and M. Stefani, *Nature*, 2002, **416**, 507–511.
4 R. Jansen, W. Dzwolak and R. Winter, *Biophys. J.*, 2005, **88**, 1344–1353.
5 J. Bieschke, J. Russ, R. P. Friedrich, D. E. Ehrnhoefer, H. Wobst, K. Neugebauer and E. E. Wanker, *Proc. Natl. Acad. Sci. U. S. A.*, 2010, **107**, 7710–7715.
6 S. Gupta, T. Chattopadhyay, M. P. Singh and A. Surolia, *Proc. Natl. Acad. Sci. U. S. A.*, 2010, **107**, 13246–13521.
7 J. Luo, S. Cao, X. Chen, S. Liu, H. Tan, W. Wu and J. Li, *Biomaterials*, 2012, **33**, 8733–8742.

8 K.-R. Cho, Y. Huang, S. Yu, S. Yin, M. Plomp, S. Qiu, R. Lakshminarayanan, J. Moradian-Oldak, M.-S. Sy and J. J. De Yoreo, *J. Am. Chem. Soc.*, 2011, **133**, 8586–8593.
9 C. Du, G. Falini, S. Fermani, C. Abbott and J. Moradian-Oldak, *Science*, 2005, **307**, 1450–1454.
10 C. L. Chen, K. M. Bromley, J. Moradian-Oldak and J. J. De Yoreo, *J. Am. Chem. Soc.*, 2011, **133**, 17406–17413.
11 K. M. Bromley, A. S. Kiss, S. B. Lokappa, R. Lakshminarayanan, D. Fan, M. Ndao, J. S. Evans and J. Moradian-Oldak, *J. Biol. Chem.*, 2011, **286**, 34643–34653.
12 S. Svenson and D. A. Tomalia, *Adv. Drug Delivery Rev.*, 2005, **57**, 2106–2129.
13 J. Li, J. Yang, J. Li, L. Chen, K. Liang, W. Wu, X. Chen and J. Li, *Biomaterials*, 2013, **34**, 6738–6747.
14 R. Esfand and D. A. Tomalia, *Drug Discovery Today*, 2001, **6**, 427–436.
15 U. Boas and P. M. H. Heegaard, *Chem. Soc. Rev.*, 2004, **33**, 43–63.
16 L. C. Palmer, C. J. Newcomb, S. R. Kaltz, E. D. Spoerke and S. I. Stupp, *Chem. Rev.*, 2008, **108**, 4754–4783.
17 D. A. Tomalia, A. M. Naylor and W. A. Goddard III, *Angew. Chem., Int. Ed.*, 1990, **29**, 138–175.
18 S. Yang, H. He, L. Wang, X. Jia and H. Feng, *Chem. Commun.*, 2011, **47**, 10100–10102.
19 Y. Li, H. He, X. Jia, W. Lu, J. Lou and Y. Wei, *Biomaterials*, 2012, **33**, 3899–3908.
20 S. Biswas, P. P. Deshpande, G. Navarro, N. S. Dodwadkar and V. P. Torchilin, *Biomaterials*, 2013, **34**, 1289–1301.
21 Q. Zhang, N. Wang, T. Xu and Y. Cheng, *Acta Biomater.*, 2012, **8**, 1316–1322.
22 K. Borowska, S. Wolowiec, K. Glowniak, E. Sieniawska and S. Radej, *Int. J. Pharm.*, 2012, **436**, 764–770.
23 K. Siewiera and M. Labieniec-Watala, *Int. J. Pharm.*, 2012, **430**, 258–265.
24 K. Karolczak, S. Rozalska, M. Wieczorek, M. Labieniec-Watala and C. Watala, *Int. J. Pharm.*, 2012, **436**, 508–518.
25 J. M. J. Fréchet, *Proc. Natl. Acad. Sci. U. S. A.*, 2002, **99**, 4782–4787.
26 S. C. Zimmerman and L. J. Lawless, *Top. Curr. Chem.*, 2001, **217**, 95–120.
27 F. Zeng and S. C. Zimmerman, *Chem. Rev.*, 1997, **97**, 1681–1712.
28 G. Doni, M. A. Kostiainen, A. Danani and G. M. Pavan, *Nano Lett.*, 2011, **11**, 723–728.
29 M. Zheng, G. M. Pavan, M. Neeb, A. K. Schaper, A. Danani, G. Klebe, O. M. Merkel and T. Kissel, *ACS Nano*, 2012, **6**, 9447–9454.
30 M. Garzoni, N. Cheval, A. Fahmi, A. Danani and G. M. Pavan, *J. Am. Chem. Soc.*, 2012, **134**, 3349–3357.
31 A. Fahmi, D. Appelhans, N. Cheval, T. Pietsch, C. Bellmann, N. Gindy and B. Voit, *Adv. Mater.*, 2011, **23**, 3289–3293.
32 T. Pietsch, N. Cheval, D. Appelhans, N. Gindy, B. Voit and A. Fahmi, *Small*, 2011, **7**, 221–225.
33 D. A. Tomalia, *Soft Matter*, 2010, **6**, 456–474.
34 D. A. Tomalia, *New J. Chem.*, 2012, **36**, 264–281.
35 D. A. Tomalia, *J. Nanopart. Res.*, 2009, **11**, 1251–1310.
36 M. J. Jasmine and E. J. Prasad, *J. Phys. Chem. B*, 2010, **114**, 7735–7742.
37 B. Lohse, M. T. Ivanov, J. W. Andreasen, R. Vestberg, S. Hvilsted, R. H. Berg, P. S. Ramanujam, C. J. Hawker and K. Mortensen, *Macromolecules*, 2007, **40**, 1779–1781.
38 X. Luo and T. Imae, *J. Mater. Chem.*, 2007, **17**, 567–571.
39 X. Shi, T. P. Thomas, L. A. Myc, A. Kotlyar and J. R. Baker, *Phys. Chem. Chem. Phys.*, 2007, **9**, 5712–5720.
40 D. Yan, Y. Zhou and J. Hou, *Science*, 2004, **303**, 65–67.
41 T. Lu, F. Han, Z. Li and J. Huang, *Langmuir*, 2006, **22**, 2045–2049.
42 G. M. Pavan and A. Danani, *J. Drug Delivery Sci. Technol.*, 2012, **22**, 83–89.
43 P. A. Akcora, H. Liu, S. K. Kumar, J. Moll, Y. Li, B. C. Benicewicz, L. S. Schadler, D. Acehan, A. Z. Panagiotopoulos, V. Pryamitsyn, V. Ganesan, J. Ilavsky, P. Thiyagarajan, P. H. Colby and J. F. Douglas, *Nat. Mater.*, 2009, **8**, 354–359.
44 D. Wu, J. Yang, J. Li, L. Chen, B. Tang, X. Chen, W. Wu and J. Li, *Biomaterials*, 2013, **34**, 5036–5047.